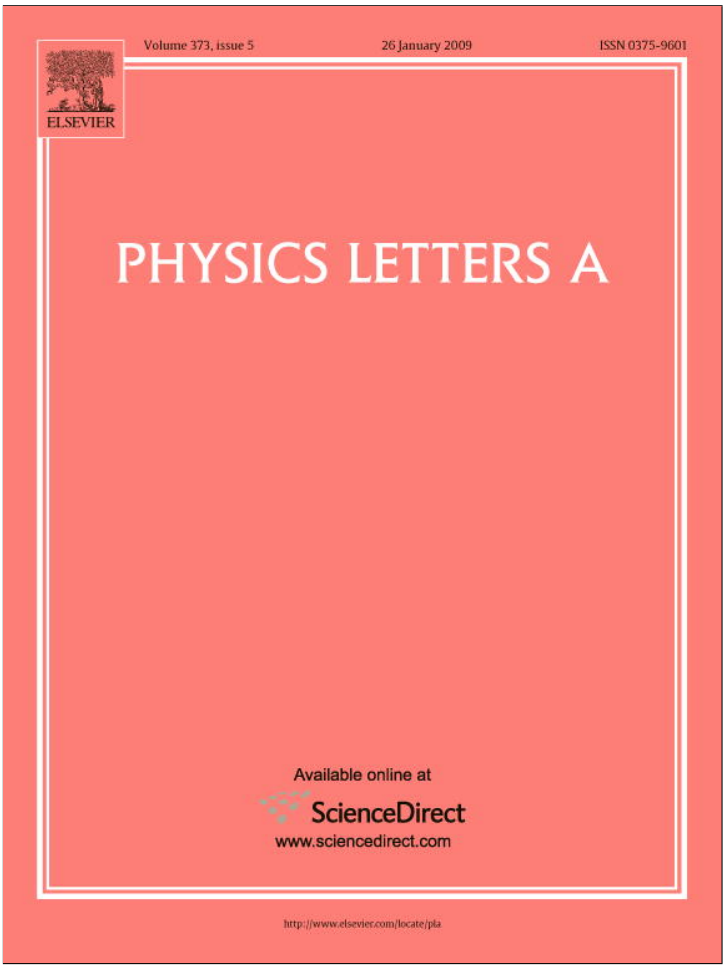

Physics Letters A 373 (2009) 525–528

Contents lists available at ScienceDirect

Physics Letters A

www.elsevier.com/locate/pla

Bound electron states in the monolayer gapped graphene with the short-range impurities

Natalie E. Firsova [a], Sergey A. Ktitorov [b,*], Philip A. Pogorelov [c]

[a] Institute for Problems of Mechanical Engineering, the Russian Academy of Sciences, St. Petersburg 199178, Russia
[b] A.F. Ioffe Physical–Technical Institute, the Russian Academy of Sciences, St. Petersburg, Russia
[c] St. Petersburg State University, Pervogo Maya str. 100, Petrodvoretz, St. Petersburg 198504, Russia

ARTICLE INFO

Article history:
Received 19 November 2008
Received in revised form 1 December 2008
Accepted 2 December 2008
Available online 14 December 2008
Communicated by V.M. Agranovich

ABSTRACT

Bound electron states in impure graphene with the massive Dirac spectrum are considered. Short-range perturbations for defect and impurities of the types "local chemical potential" and "local gap" are taken into account.

1. Introduction

The Dirac equation is a fundamental base of the relativistic field theory. However, it is an important model in the non-relativistic solid state theory as well. Superconductors with d-pairing [1], the Cohen–Blount two-band model of narrow-gap semiconductors [2,3], electronic spectrum of the carbon tubes form an incomplete list of the non-relativistic applications of this equation. During the last two years extremely much attention was payed to the problem of the electronic spectrum of graphene (see for the review [5]). Two-dimensional structure of it and a presence of the cone points in the electronic spectrum make actual a comprehensive study of the external fields effect on the spectrum and other characteristics of the electronic states described by the Dirac equation in the $2+1$ space–time. We consider in this work the bound states of the $2+1$ gapped Dirac equation due to the short-range perturbation. The pristine graphene is gapless, but violation of symmetry between the sublattices can induce opening of the gap [4]. The symmetry violation can be triggered by the substrate or be developed dynamically. Notice that "short-range" stands here for the lack of a long-range tail of the potential. At the same time the perturbation radius remains finite that is equivalent to the large quasi momentum cut-off [3]. This cut-off makes the quasi-momentum space form-factors of the perturbation small enough for the quasi-momentum transfer of the order of the reciprocal lattice vector and, therefore, mixing of K and K' states can be done non-effective (this mixing was studied in [6] and [7]). Particular attention to the short-range perturbation case stems from the effectiveness of short-range scatterers in contrast to the long-range ones: an effect of the latter is suppressed by the Klein paradox [8]. Our work takes into account the obvious fact that the Kohn–Luttinger matrix elements of the short-range perturbation calculated on the upper and lower band wave functions are not equal in a general case. This means that in the perturbed Dirac equation not only the potential but the mass perturbation can be present.

2. Perturbed Dirac equation in $(2+1)$-space–time

The Dirac equation describing electronic states in graphene reads [5]

$$\left(-is\hbar\sum_{\mu=1}^{2}\sigma_\mu\partial_\mu-\sigma_3(m+\delta m)s^2\right)\psi=(E-V)\psi, \tag{1}$$

where s is the limiting velocity of the band electrons, σ_μ are the Pauli matrices, $2ms^2=E_g$ is the electronic spectrum gap, $\psi(\mathbf{r})$ is the two-component spinor. The spinor structure takes into account the two-band nature. $\delta m(\mathbf{r})$ and $V(\mathbf{r})$ are the local perturbations of the mass (gap) and the chemical potential. A local mass perturbation can be induced by defects in the graphene film or in the substrate [9]. We consider here the delta function model of the perturbation:

$$\delta m(\mathbf{r})=-b\delta(r-r_0),\qquad V(\mathbf{r})=-a\delta(r-r_0), \tag{2}$$

where r and r_0 are respectively the polar coordinate radius and the perturbation radius. Such short-range perturbation (and the equivalent form $\mathrm{diag}(V_1,V_2)\delta(r-r_0)$ with $-V_1=\frac{a+b}{2}$, $-V_2=\frac{a-b}{2}$) was used in the $(3+1)$-Dirac problem for narrow-gap and zero-gap semiconductors in [3]. The two-dimensional Dirac problem with the scalar short-range perturbation (2) (but without the mass perturbation) was considered in [10]. The obtained there characteristic equation for the discrete spectrum energy contains one mistake. We correct it here and take account of the mass perturbation $\delta m(\mathbf{r})$.

* Corresponding author.
E-mail address: ktitorov@mail.ioffe.ru (S.A. Ktitorov).

0375-9601/$ – see front matter
doi:10.1016/j.physleta.2008.12.014

Let us present the two-component spinor in the form

$$\psi_j(\mathbf{r},t)=\frac{\exp(-iEt)}{\sqrt{r}}\begin{pmatrix} f_j(r)\exp[i(j-1/2)\phi] \\ g_j(r)\exp[i(j+1/2)\phi]\end{pmatrix}, \tag{3}$$

where j is the pseudospin quantum number; $j=\pm 1/2, \pm 3/2, \ldots$. In the opposite to the relativistic theory, this quantum number has nothing to do with the real spin and indicates the degeneracy in the biconic Dirac point. The upper $f_j(r)$ and $g_j(r)$ components of the spinor satisfy the equations

$$\frac{dg_j}{dr}+\frac{j}{r}g_j-(E-m)f_j=(a+b)\delta(r-r_0)f_j, \tag{4}$$

$$-\frac{df_j}{dr}+\frac{j}{r}f_j-(E+m)g_j=(a-b)\delta(r-r_0)g_j. \tag{5}$$

These equations have a symmetry:

$$f_j\leftrightarrow g_j,\qquad E\to -E,\qquad j\to -j. \tag{6}$$

Let us introduce the function $\varphi_j(r)\equiv f_j/g_i$. It satisfies the equation:

$$\frac{1}{(a+b)\varphi_j^2+(a-b)}\left[\frac{d\varphi_j}{dr}-\frac{2j}{r}\varphi_j-E\left(\varphi_j^2+1\right)\right] +\delta(r-r_0)=0. \tag{7}$$

Integrating in the vicinity of $r=r_0$

$$\lim_{\epsilon\to 0}\int\limits_{\varphi_j(r_0-\epsilon)}^{\varphi_j(r_0+\epsilon)}\frac{d\varphi_j}{(a+b)\varphi_j^2+(a-b)}=-1, \tag{8}$$

we obtain the matching condition

$$\arctan\left(\varphi_j^-\sqrt{\frac{a+b}{a-b}}\right)-\arctan\left(\varphi_j^+\sqrt{\frac{a+b}{a-b}}\right)=\sqrt{a^2-b^2}, \tag{9}$$

where $\varphi_j^-\equiv\varphi_j(r_0-\epsilon)$, $\varphi_j^+\equiv\varphi_j(r_0+\epsilon)$, $a^2>b^2$. The upper and lower component matching condition resulting from (9) reads

$$\begin{pmatrix} f_j^+ \\ g_j^+\end{pmatrix}=\hat{A}\begin{pmatrix} f_j^- \\ g_j^-\end{pmatrix}, \tag{10}$$

where the matrix $\hat{A}$

$$\begin{pmatrix} \cos\sqrt{a^2-b^2} & -\sqrt{\frac{a-b}{a+b}}\sin\sqrt{a^2-b^2} \\ \sqrt{\frac{a-b}{a+b}}\sin\sqrt{a^2-b^2} & \cos\sqrt{a^2-b^2}\end{pmatrix} \tag{11}$$

is orthogonal for $b=0$. It transmutes into the matrix

$$\begin{pmatrix} \cosh\sqrt{b^2-a^2} & -\sqrt{\frac{b-a}{b+a}}\sinh\sqrt{b^2-a^2} \\ \sqrt{\frac{b-a}{b+a}}\sinh\sqrt{b^2-a^2} & \cosh\sqrt{b^2-a^2}\end{pmatrix}, \tag{12}$$

when $a^2-b^2<0$.

The general solution can be found solving the second-order equation obtained by excluding one of the spinor components from the equation set (4), (5) in the domains $0<r<r_0$ and $r>r_0$:

$$\frac{d^2f_j}{dr^2}+\left[E^2-m^2-\frac{j(j-1)}{r^2}\right]f_j=0. \tag{13}$$

This equation is related to the Bessel one. Its general solution reads

$$f_j=C_1\sqrt{r}I_{j-1/2}(\kappa r)+C_2\sqrt{r}K_{j-1/2}(\kappa r), \tag{14}$$

where $\kappa^2=m^2-E^2$, $I_\nu(z)$ and $K_\nu(z)$ are the modified Bessel functions. The constant $C_2=0$ in the domain $0<r<r_0$, while $C_1=0$ in the domain $r>r_0$. Expressing the g_j-component using (5), we can write

$$\varphi_j^-=\sqrt{\frac{m+E}{m-E}}\frac{I_{j-1/2}(\kappa r_0)}{I_{j+1/2}(\kappa r_0)}, \tag{15}$$

$$\varphi_j^+=\sqrt{\frac{m+E}{m-E}}\frac{K_{j-1/2}(\kappa r)}{K_{j+1/2}(\kappa r)}. \tag{16}$$

Applying the matching condition (9) to the expressions (16), (15) we obtain the characteristic equation for the bound state energy levels:

$$\begin{aligned}&\kappa\left[\frac{K_{j-1/2}(\kappa r_0)}{K_{j+1/2}(\kappa r_0)}-\frac{I_{j-1/2}(\kappa r_0)}{I_{j+1/2}(\kappa r_0)}\right] \\ &\quad=-\frac{\tan(\sqrt{a^2-b^2})}{\sqrt{a^2-b^2}}\left[(m-E)(a-b)\right. \\ &\qquad\left.+(a+b)(m+E)\frac{I_{j-1/2}(\kappa r_0)}{I_{j+1/2}(\kappa r_0)}\frac{K_{j-1/2}(\kappa r_0)}{K_{j+1/2}(\kappa r_0)}\right]\end{aligned} \tag{17}$$

where $a^2-b^2>0$. This equation turns to the characteristic equation obtained in [10], for $b=0$ apart from the mistakenly omitted terms in the right-hand side of (17). In the opposite case of $a^2-b^2<0$ we have

$$\begin{aligned}&\kappa\left[\frac{K_{j-1/2}(\kappa r_0)}{K_{j+1/2}(\kappa r_0)}-\frac{I_{j-1/2}(\kappa r_0)}{I_{j+1/2}(\kappa r_0)}\right] \\ &\quad=-\frac{\tanh(\sqrt{b^2-a^2})}{\sqrt{b^2-a^2}}\left[-(m-E)(b-a)\right. \\ &\qquad\left.+(b+a)(m+E)\frac{I_{j-1/2}(\kappa r_0)}{I_{j+1/2}(\kappa r_0)}\frac{K_{j-1/2}(\kappa r_0)}{K_{j+1/2}(\kappa r_0)}\right].\end{aligned} \tag{18}$$

We write these equations in another form making the symmetry (6) manifest:

$$\begin{aligned}&\kappa\left[I_{j-1/2}(\kappa r_0)K_{j+1/2}(\kappa r_0)-K_{j-1/2}(\kappa r_0)I_{j+1/2}(\kappa r_0)\right] \\ &\quad=\frac{\tan(\sqrt{a^2-b^2})}{\sqrt{a^2-b^2}}\left[(m-E)(a-b)I_{j+1/2}(\kappa r_0)K_{j+1/2}(\kappa r_0)\right. \\ &\qquad\left.+(a+b)(m+E)I_{j-1/2}(\kappa r_0)K_{j-1/2}(\kappa r_0)\right],\end{aligned} \tag{19}$$

$$\begin{aligned}&\kappa\left[I_{j-1/2}(\kappa r_0)K_{j+1/2}(\kappa r_0)-K_{j-1/2}(\kappa r_0)I_{j+1/2}(\kappa r_0)\right] \\ &\quad=\frac{\tanh(\sqrt{b^2-a^2})}{\sqrt{b^2-a^2}}\left[-(m-E)(b-a)I_{j+1/2}(\kappa r_0)K_{j+1/2}(\kappa r_0)\right. \\ &\qquad\left.+(b+a)(m+E)I_{j-1/2}(\kappa r_0)K_{j-1/2}(\kappa r_0)\right].\end{aligned} \tag{20}$$

3. Analysis of the characteristic equation and numerical results

Making use of the Bessel functions limiting forms for small arguments [11]

$$I_\nu(z)\sim(z/2)^\nu\frac{1}{\Gamma(\nu+1)},\qquad K_0(z)\sim-\ln z,$$

$$K_\nu(z)\sim\frac{1}{2}\Gamma(\nu)(z/2)^{-\nu},$$

we can obtain a simple relation describing the asymptotic behaviour of the energy level, where the perturbation power approaches zero:

$$E=m\left[1-\frac{r_c^2}{2r_0^2}\exp\left(-\frac{r_c}{r_0(a+b)}\right)\right], \tag{21}$$

where $r_c=m^{-1}$ (in units with $\hbar=s=1$), $a+b>0$. This result conforms the well known general property of the two-dimensional quantum systems: a threshold for creation of the bound state is absent; the point $a+b=0$ is the essentially singular point of the function $E=E(a+b)$. One can see that the function $E(a)$ approaches the point $E=-m$ at some large enough value of $a>0$. Making use of the Bessel function asymptotic behaviour [11],

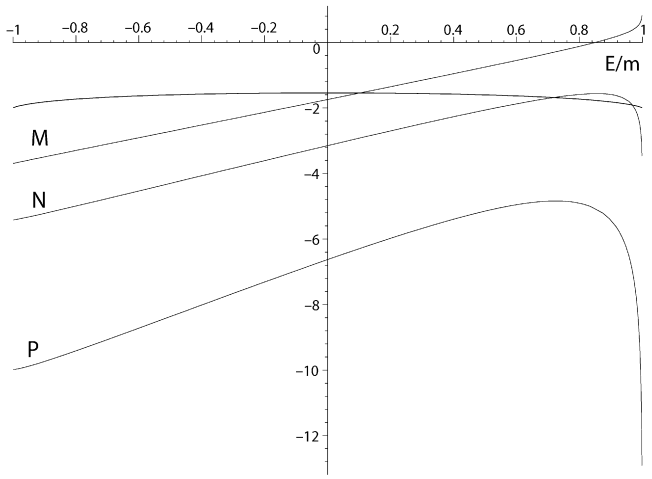

Fig. 1. Graphical solution of the characteristic equation (17). It illustrates three various possibilities for different a magnitudes $(0.93; 1.23; 1.53)$ and fixed $b = -1$: M: one energy eigenvalue; N: two energy eigenvalues; P: no energy eigenvalues within the gap.

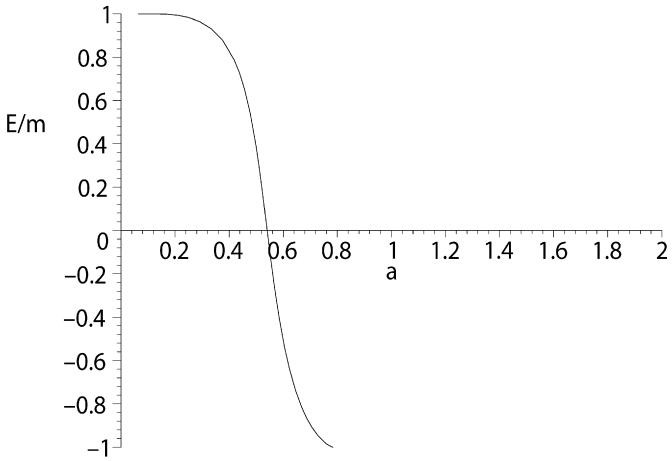

Fig. 2. Reduced lower electron bound state energy E/m dependence on the short-range potential amplitude a at $b = 0$.

$$I_\nu(z) \sim (2\pi z)^{-1/2} \exp z, \qquad K_\nu(z) \sim \left(\frac{\pi}{2z}\right)^{1/2} \exp(-z),$$

and Eq. (18), we can see that the function $E(b)$ approaches the point $E = 0$, when $\frac{r_0}{r_c}$ is large enough and $b \to \infty$.

Graphical solution of the characteristic equation (17) is presented in Fig. 1. It illustrates three various possibilities for different a magnitudes $(0.93; 1.23; 1.53)$ and fixed $b = -1$: M stands for one eigenvalue; N stands for two eigenvalues; P stands for absence of eigenvalues within the gap.

In Fig. 2, the electron bound state energy is presented as a function of the potential amplitude for the angular momentum quantum number values $j = 1/2$, $\frac{r_0}{r_c} = 1$ and $b = 0$. Inspecting this plot one can see that our analytic solution (21) perfectly approximates approaching of the bound state energy value the upper band bottom, when b approaches zero.

In Fig. 3, the bound state energy is presented as a function of the mass perturbation amplitude b for $a = 0$, $\frac{r_0}{r_c} = 1$, $j = 1/2$.

In Fig. 4, the electron bound state energy is presented as a function of the potential amplitude for the angular momentum quantum number $j = 1/2$, $\frac{r_0}{r_c} = 1$, and $b = -1$. We see that the energy dependence on a is non-monotonic function, but approaching the upper band bottom takes place similarly to the case of $b = 0$. Points M, N, P correspond to eigenvalues depicted in Fig. 1.

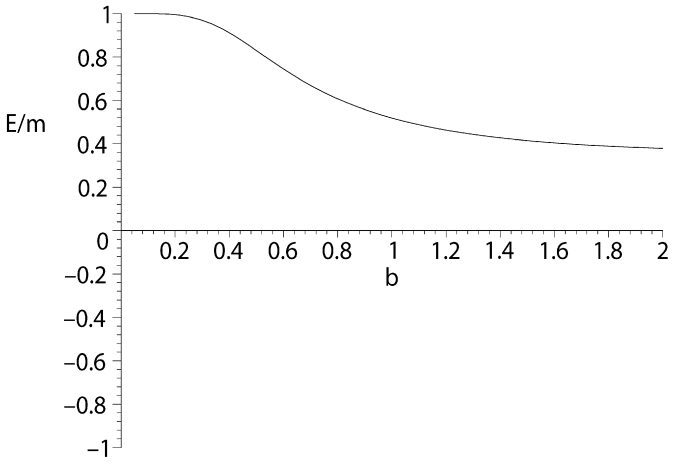

Fig. 3. Reduced lower electron bound state energy E/m dependence on the mass perturbation amplitude b at $a = 0$.

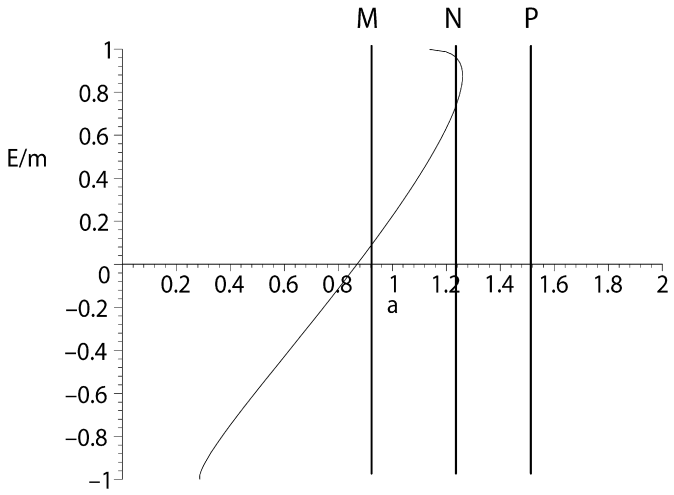

Fig. 4. Reduced lower electron bound state energy E/m dependence on the short-range potential amplitude a at $b = -1$. Points M, N, P correspond to eigenvalues depicted in Fig. 1.

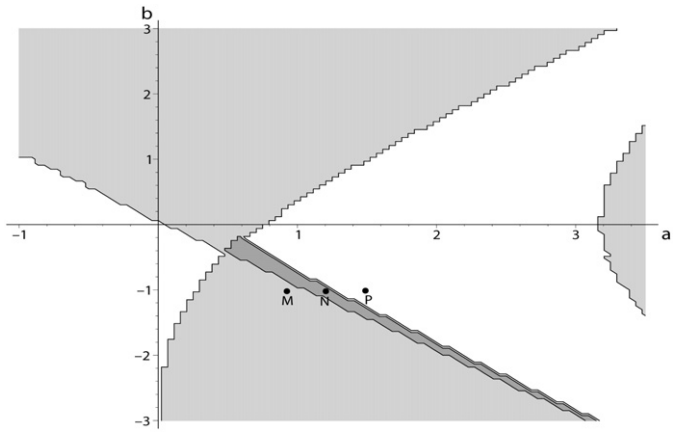

Fig. 5. Distribution of bound states number in (a, b) plane for $j = 1/2$. Points M, N, P stand respectively for one, two and zero crossings shown in Fig. 1.

Distribution of the bound states number in the (a, b) plane for $j = 1/2$ is depicted in Fig. 5. Points M, N, P stand respectively for one, two and zero crossings shown in Fig. 1. It is seen from our figures that simultaneous existence of two bound states is possible within the narrow segment in the plane (a, b).

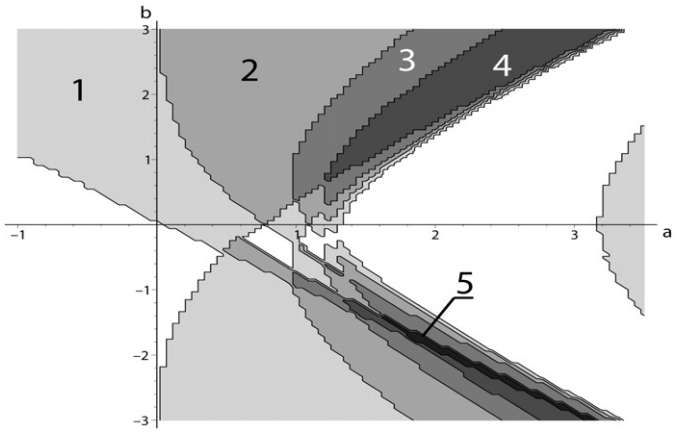

Fig. 6. Distribution of bound states number in (a, b) plane for $j = 1/2; 3/2; 5/2; 7/2$.

Distribution of bound states number in (a, b) plane for $j = 1/2; 3/2; 5/2; 7/2$ is presented in Fig. 6. Solutions for negative j are easy to obtain from the symmetry $E \to -E$, $j \to -j$, $a \to -a$.

4. Conclusion

In conclusion, we considered the bound electron states for the two-dimensional Dirac equation with the short-range perturbation. The short-range perturbation is approximated by the delta function $\delta(r - r_0)$ with different amplitudes in the upper and lower bands. We found the characteristic equation for the discrete energy levels. Energy levels behaviour in dependence on the perturbation amplitudes was investigated both analytically and numerically. The structure of our characteristic equations allows us to make the following general conclusions. The energy spectrum is a periodic function of a for $b = 0$. In the case of finite value of a and $b \to \infty$, $\tanh(\sqrt{b^2 - a^2}) \to 1$ and, therefore, $E \to$ const. Notice that the bound states energy levels obtained in the case of the vanishing parameter b are in the qualitative correspondence to the energy levels deduced from the scattering amplitude poles calculated in [12]. The obtained results can be useful for understanding of the graphene electron properties.

References

[1] D.J. Scalapino, Phys. Rep. 250 (1995) 329.
[2] L.V. Keldysh, JETP 45 (1963) 365.
[3] S.A. Ktitorov, V.I. Tamarchenko, Sov. Phys. (Solid State) 19 (1977) 2070.
[4] S.Y. Zhou, G.H. Gweon, A.V. Fedorov, et al., Nature Mater. 6 (2008) 770.
[5] A.H. Castro Neto, F. Guinea, et al., arXiv: 0709.1163, 2008.
[6] I.L. Aleiner, K.B. Efetov, Phys. Rev. Lett. 97 (2006) 236801.
[7] D.M. Basko, Phys. Rev. B 78 (2008) 115432.
[8] C.W.J. Beenakker, Rev. Mod. Phys. 80 (2008) 1337.
[9] A. Lherbier, X. Blaze, et al., Phys. Rev. Lett. 101 (2008) 036808.
[10] S.-H. Dong, Z.-Q. Ma, Found. Phys. Lett. 15 (2002) 171.
[11] M. Abramowitz, I.A. Stegun, Handbook of Mathematical Functions with Formulas, Graphs, and Mathematical Tables, National Bureau of Standards, Washington, DC, 1964.
[12] D.S. Novikov, Phys. Rev. B 76 (2007) 245435.